Heliyon 9 (2023) e17082

Contents lists available at ScienceDirect

Heliyon

journal homepage: www.cell.com/heliyon

Metformin-loaded nanoerythrosomes: An erythrocyte-based drug delivery system as a therapeutic tool for glioma

Seyed Mohammad Iman Moezzi [a,b], Parisa Javadi [c], Negin Mozafari [b], Hajar Ashrafi [b], Amir Azadi [b,d,*]

[a] Student Research Committee, Shiraz University of Medical Sciences, Shiraz, Iran
[b] Department of Pharmaceutics, School of Pharmacy, Shiraz University of Medical Sciences, Shiraz, Iran
[c] Department of Nanomedicine, School of Novel Medical Sciences and Technologies, Shiraz University of Medical Sciences, Shiraz, Iran
[d] Pharmaceutical Sciences Research Center, Shiraz University of Medical Sciences, Shiraz, Iran

A B S T R A C T

Glioma is an intra-cranial malignancy with the origin of neural stem cells or precursor cells, the most prevalent brain tumor worldwide. Glioblastoma, the fourth-grade glioma, is a common brain tumor whose incidence rate is 5–7 people per 100,000 populations annually. Despite their high mortality rate, all efforts for treatment have yet to achieve any desirable clinical outcome. The Wnt signaling pathway is a conserved pathway among species that seems to be a candidate for cancer therapy by its inhibition. Metformin is a known inhibitor of the Wnt signaling pathway. Its effects on glioma treatment have been observed in cellular, animal, and clinical experiments. Nanoerythrosomes are drug carriers obtained from the cellular membrane of red blood cells in nano size which can offer several characteristics to deliver metformin to brain tumors. They are good at loading and carrying hydrophilic drugs, they can protect metformin from its metabolizing enzymes, which are present in the blood-brain barrier, and they can extend the period of metformin presence in circulation. In this study, nanoerythrosomes were prepared by using the hypotonic buffer. They had particle sizes in the range of 97.1 ± 34.2 nm, and their loading efficiency and loading capacity were 72.6% and 1.66%, respectively. Nanoerythrosomes could reserve metformin in their structure for a long time, and only 50% of metformin was released after 30 h. Moreover, they released metformin at a low and approximately constant rate. Besides, nanoerythrosomes could tolerate various kinds of stress and maintain most of the drug in their structure. Altogether, nanoerythrosome can be a suitable drug delivery system to deliver therapeutic amounts of metformin to various tissues.

1. Introduction

Glioma is an intra-cranial neuro-epithelial malignancy whose origin is glial cells. Glial cells are some un-neuronal cells that reside in the central nervous system (CNS), and their role is to protect, nourish, and support neural cells [1]. Glial cells mainly include astrocytes, oligodendrocytes, and ependymal cells [2]. Glioma is the most prevalent brain tumor, with a survival time of approximately 14.6 months for patients [3]. Its incidence rate varies based on histopathology, age, sex, and differences in diagnosis. Even though, it is

Abbreviations: ABCB1, ATP-binding cassette B1; AIC, Akaike's information criterion; Akt, Protein kinase B; AMPK, AMP-activated protein kinase; BBB, Blood-brain barrier; CYP, Cytochrome P450; DLS, Differential light scattering; EPR, Enhanced permeation and retention effect; LD-PSA, LASER diffraction article size analyzer; LDL, Low-density lipoprotein; MAPK, Mitogen-activated protein kinase; mTOR, Mechanistic target of rapamycin; PCP, Planar cell polarity; PDI, Poly-dispersity index; PI3K, Phosphoinositide 3-kinase; SEM, Scanning electron microscopy; Sox4, SRY-Box transcription factor 4; STAT, Signal transducer and activator of transcription; TEM, Transmission electron microscopy; Wnt, Wingless-related integration site.

* Corresponding author. Department of Pharmaceutics, School of Pharmacy, Shiraz University of Medical Sciences, Shiraz, Iran.
E-mail address: aazadi@sums.ac.ir (A. Azadi).

https://doi.org/10.1016/j.heliyon.2023.e17082
Received 14 May 2023; Received in revised form 6 June 2023; Accepted 7 June 2023
Available online 7 June 2023

estimated that the age-adjusted incidence rate of glioma is about 4.67–5.73 per 100,000 people each year [4]. Moreover, glioblastoma has also been shown to have an incidence rate of about 5–7 per 100,000 people [5]. The main protocol for both glioma and glioblastoma treatment is surgery accompanied by chemotherapy or radiotherapy. In glioblastoma, the mean overall survival and 5-year survival of radiotherapy are 9–10 months and 1.9%, respectively.

Various signaling pathways are active in the glioma pathogenesis, growth, and progress phenomena such as metastasis, stemness, invasion, immortality, drug resistance, and angiogenesis. Among these pathways, the calcium signaling pathway, MAPK signaling, mTOR signaling, p53 signaling, and ErbB signaling pathways could be mentioned. Specifically, the Wnt signaling pathway is a highly conserved pathway among different species with diverse effects on cancer pathogenesis [6]. Wingless-related integration site (Wnt) gene was first introduced as a marker in mice breast tumors and related to the wingless phenotype of drosophila [7]. Its significant role in developing and differentiating CNS structures has been shown vividly [8]. The Wnt signaling pathway is mainly divided into two canonical and non-canonical pathways (Non-canonical pathway is classified into planar cell polarity (PCP) and Wnt/Calcium pathways). In the canonical Wnt pathway, β-catenin plays an important role, so it is called the β-catenin-dependant pathway [9]. Wnt3a, Wnt5a, and Wnt7a are the three main members of the Wnt family and ligands of this signaling pathway. Wnt7a, which exists in both canonical and PCP pathways, is a key role-player in cancer pathogenesis [10]. Wnt signaling has various roles in malignancy-related mechanisms such as stemness, invasion, drug resistance, and angiogenesis. Specifically, the role of Wnt signaling in glioma has been studied well. FAT1 is a protein member of the protocadherins family that inhibits β-catenin activity as a transcription factor. It is shown that 57% of glioblastoma cases are null for the FAT1 gene [11]. Hepatocyte growth factor (HGF) and its receptor (c-Met) are important proteins in the pathogenesis of glioblastoma, and their overexpression is related to the disease's poor prognosis. In glioma stem cells when the c-Met expression is higher, the Wnt signaling is more active. Also, the inhibition of c-Met would reduce transportation of

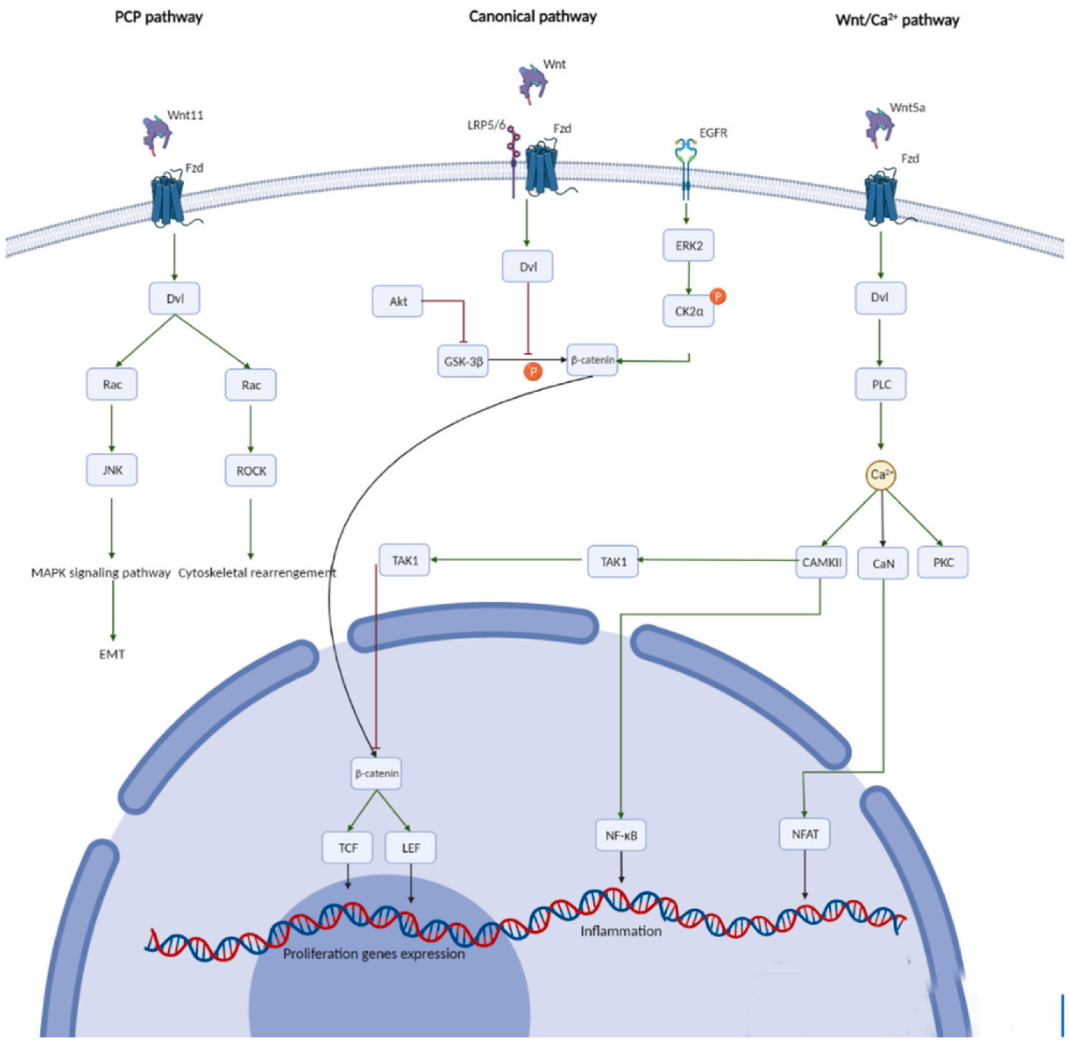

Fig. 1. Wnt signaling pathway in glioma (Created by BioRender.com). The non-canonical Wnt signaling pathway has two independent subdivisions, planar cell polarity (PCP) and Wnt/Ca^{2+} pathways. The PCP signaling controls the polarity of the cell in the basal membrane. Wnt/Ca^{2+} pathway is the regulator of calcium trafficking from the endoplasmic reticulum to the cytosol [45].

β-catenin to the nucleus in glioblastoma cells [12]. The Wnt signaling pathway is believed to correlate with the proliferation and survival of glioma stem cells, too. In glioblastoma, the enhanced expression of the pleiomorphic adenoma gene like-2 (PLAGL-2) gene will activate the Wnt/β-catenin signaling pathway in neural stem cells and make glioma stem cells renew (Fig. 1) [13].

Oral temozolomide is a widely used drug that is the best anticancer agent for glioma despite its trivial clinical outcomes. Adding temozolomide to the radiotherapy would increase the mean overall survival and 5-year survival to 14 months and 10.9%, respectively [14]. Unfortunately, the clinical outcomes of temozolomide cannot be seen in 50% of patients due to the resistance [14]. Surprisingly, Wnt has a crucial role in glioblastoma resistance to temozolomide [15]. Besides, ABCB1, responsible for the efflux of drugs from tumor cells and presents in 70%–100% of high-grade gliomas, is regulated by Wnt5a [16]. This evidence suggests inhibition of Wnt signaling as a potential therapeutic strategy to confront glioma. Other medications are biodegradable carmustine-loaded wafer (Gliadel®) [17], the combination therapy of radiotherapy and procarbazine, lomustine, and vincristine (PCV) [18], and bevacizumab [19]. However, each has its own limitations with little clinical significance [14]. Various limitations for recent anti-glioma drugs have been counted. Many anticancer drugs cannot cross the BBB or reach the therapeutic concentration in the brain tissue. Because of their systemic administration, they distribute in every organ and cause serious side effects, such as bone marrow suppression [20]. As a result, repositioning a safer drug for glioma treatment and designing a drug delivery system that can target glioma tumors that preserves the drug from wide distribution would be a dream for treating glioma.

Metformin is a known and approved Wnt signaling pathway inhibitor, making it a promising candidate for repositioning to treat glioma. Metformin is the first line of oral therapy for type 2 diabetes, and it has been suggested in different guidelines for different cancers, obesity, and even Alzheimer's disease [21]. Its effect on Wnt signaling has been investigated in various studies. Metformin downregulated β-catenin in endometrium cancer which seems independent of the AMPK pathway [22]. Another study showed that metformin can reduce Dvl3 and, consequently, β-catenin by activating the AMPK pathway. This suppressed the growth of cervical cancer cells [23]. Similarly, Amable et al. found that metformin can inhibit phosphorylation and activation of β-catenin through AMPK/PI3K/Akt pathway [24]. The effect of metformin in the decrease of inflammation and Wnt suppression has also been shown in pancreatic cancer [25]. Moreover, the effect of metformin on glioma has been investigated. Metformin can regulate mitochondrial anabolism, cease the cell cycle, induce cell death, and resensitize glioma cells to temozolomide. It has been shown that metformin reduces the proliferation and migration of glioma-initiating cells, independent of its TGF-β-inhibiting activity [26]. In one study, the effect of metformin on the reduction of invasiveness and motility of glioblastoma tumor cells through the Akt pathway has been observed [27]. It is shown that metformin has a specified cytotoxic effect on the glioma-initiating cell. Moreover, treating glioma cells with metformin resensitizes them to temozolomide [28]. Metformin can suppress the proliferation of glioma cells by activating the AMPK pathway and inhibiting the phosphorylation of STAT3 [29].

In some clinical trials, the effect of metformin on glioma has been investigated. In a retrospective study, authors concluded that monotherapy with metformin before diagnosing glioma is essential in predicting patients' survival [30]. In another study on 1093 patients with high-grade gliomas, it was shown that only grade 3 patients had more survival in response to metformin-added therapy. It is assumed that this is because of metabolic problems in grade 3 glioma that metformin helped them to improve. This effect was not observed in glioblastoma patients [31]. Conversely, a meta-analysis reported that relation between metformin administration and improved survival of glioma patients is insignificant [32]. In another study, the effect of metformin in addition to temozolomide in glioma patients was reported to be meaningless. Researchers believed the reason for this result was the low concentration of metformin in the brain of patients. While the concentration of metformin in *in-vitro* studies is in the millimolar range, its concentration in these patients' brains was in the micromolar range [32]. Moreover, it is shown that metformin metabolizing enzymes, CYP-2D1 and CYP-2C11, are present in the BBB-forming astrocytes, which can be the reason for this drop in metformin concentration [33–35]. Overall, metformin can be a valuable candidate to treat glioma through inhibition of the Wnt signaling pathway or other known or unknown mechanisms.

Nanoerythrosome is a drug carrier in nano size that is produced from the membrane of erythrocytes. Nanoeryhtrosomes preserve the characteristics of their origin as well. They are fully biocompatible and biodegradable. If the origin blood for their production would be the patient's own blood, no immunogenicity is expected. Their particle size is 100–200 nm letting them circulate freely in the vessels and cross biological barriers [36]. Nanoerythrosomes can accumulate inside the tumors through the enhanced permeation and retention (EPR) effect. Because of the loose vascular structure of tumors and their high leakage, besides their improper lymphatic system, nano-size drug carriers would preferentially extravasate through the endothelium of tumor vessels. On the other hand, in healthy tissues, due to tight junctions of the endothelium, nanoerythrosomes have much less access to normal cells and interstitial fluid [37]. Moreover, cellular drug delivery systems, including nanoerythrosomes, can induce local inflammation in the brain, disturbing the integrity of the BBB, which helps them cross the BBB [38].

Studies revealed that we might expect nanoerythrosomes to have a half-life near the erythrocyte, i.e., 120 days. Because of this long lifespan and small size, nanoerythrosomes can cross BBB and concentrate in the brain tissue [39]. The best-known strategy to deliver drugs to the brain was transferrin receptor targeting nanoparticles. Interestingly, it is observed that intra-arterial administration of erythrocyte membrane-based nanoparticles had a much better result than the last best strategy (12% of administered dose vs. 0.5–1% of it) [40].

Due to the aging process of nanoerythrosomes, their membrane will lose flexibility and integrity. This makes them destruct during passages from the delegate capillaries of the spleen. Moreover, RES macrophages, Kupfer cells of the liver, alveolar macrophages of lungs, monocytes, and endothelial cells will play roles in nanoerythrosomes elimination [41]. No toxicity has been reported from nanoerythrosomes or any RBC-derived carrier [42]. In addition, the side effects of loaded drugs would decrease because of their encapsulation in a biological membrane and reduction of free or protein-bound amounts of drug [43].

To produce a successful nanoerythrosome-based drug delivery system, it is important to choose a hydrophilic drug insensitive to

erythrocytes' active degradation mechanisms. Various drugs have been used for loading in nanoerythrosomes for different indications, among which we can mention hydrocortisone, propranolol, chlorpromazine, vinblastine, tetracaine, retinol, and capecitabine [44].

Based on the information above, the aim of the study is to design a nanoerythrosome to deliver metformin to the brain. The prepared system was evaluated based on different *in-vitro* experiments to obtain a primary insight into the characteristics of metformin-loaded nanoerythrosomes.

2. Materials and methods

2.1. Materials

Packed RBCs were obtained from the Blood Transfusion Organization. Metformin produced by Aarti Drugs Limited© company was obtained from Exir© pharmaceutical company (Borujerd, Iran). Polysorbate 80 was purchased from Merck©, Germany. Dialysis bags with a 3.5 KDa cut-off was purchased from Serva© (Germany). Phosphate buffer solution (PBS) for washes and incubations was purchased from Asagene©, (Iran).

2.2. Nanoerythrosome preparation

To produce ghost RBCs, 3 mL of packed RBC was mixed with 12 mL of hypotonic PBS (0.1X), shaken, and incubated at 4 °C for 15 min. After that, the mixture was centrifuged at 3000 rpm for 10 min. The remnant was washed 3 times with hypotonic PBS and dispersed in isotonic PBS at 4 °C for further processes.

To load metformin in the ghost RBCs, RBCs were dispersed in 0.5 mL of isotonic PBS and incubated with 0.25 mL metformin solution in PBS (0.1, 1, and 10 mg/mL) for 1 h at room temperature on the shaker. After that 1.5 mL of hypertonic PBS (10X) was added and the mixture was incubated at 4 °C for another 1 h. Finally, the mixture was centrifuged at 3000 rpm for 10 min to separate the loaded ghost RBCs and unloaded metformin. The supernatant was preserved for drug assay.

To form nanoerythrosome and reduce the particle size, after the addition of 1% v/v of polysorbate 80 and bringing up the volume to 10 mL with isotonic PBS, the metformin-loaded ghost RBCs were undergone 10 min of homogenization (Heidolph, SilentCrusher M, Germany) with 20,000 rpm and 10 min of probe sonication (Heilscer, UP200H, Germany) with 50% potency and 0.5s cycle. All of these steps are summarized in Fig. 2.

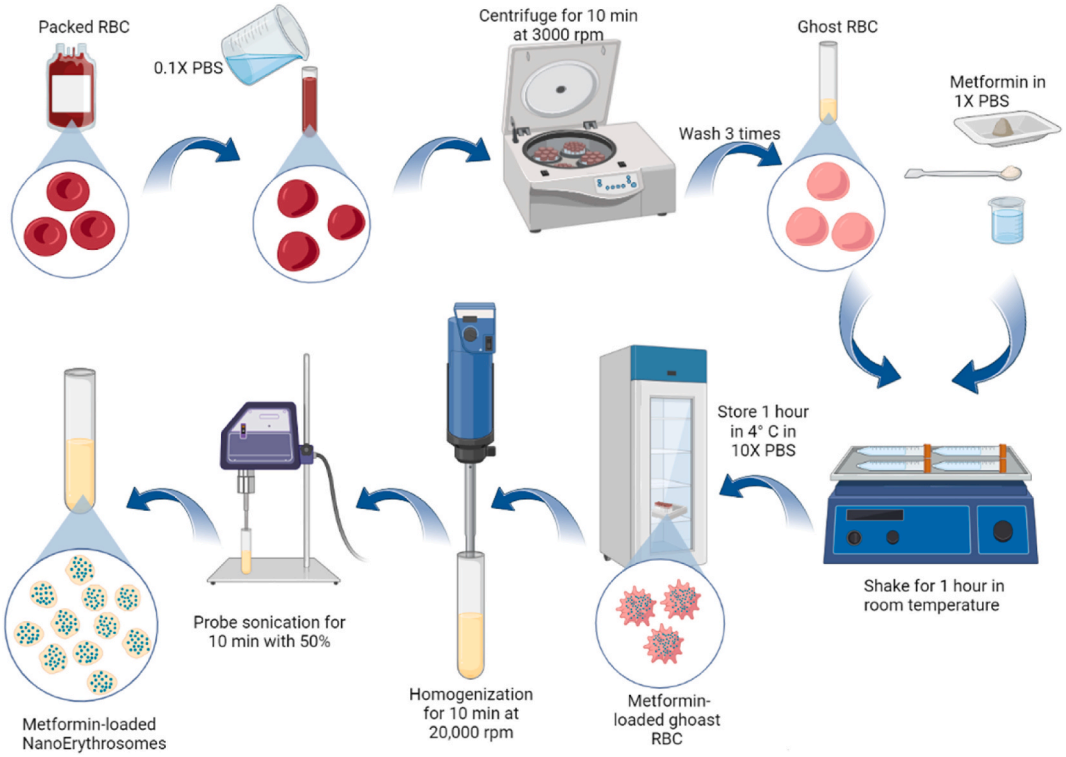

Fig. 2. A schematic representation of metformin-loaded nanoeryhrosome preparation steps (Created by BioRender.com).

2.3. Characterization of nanoerythrosomes

2.3.1. Particle size and size distribution

For particle size measurement, we used both differential light scattering (DLS) (Horiba, SZ-100, Japan) and laser diffraction particle size analyzer (LD-PSA) (Shimadzu, SALD-2101, Japan). Before each LD-PSA measurement, the samples were shaken for 30 s to disperse well. For DLS, each sample was placed in bath sonication for 5 min. The refractive index of LD-PSA was set at 1.6. For size distribution of nanoerythrosome, the span and polydispersity index has been reported.

2.3.2. Zeta potential

To evaluate the surface charge of unloaded- and loaded-nanoerythrosomes, zeta potential was measured by zetasizer (Horiba, SZ-100, Japan).

2.3.3. Shape and surface morphology

A 20 μL sample was placed on a formvar Carbon film coated on a 300 mesh copper grid (EMS) for 2 min. Excess liquid was absorbed with filter paper and then negatively stained with a 20 μL drop of 2% uranyl acetate for 1–2 min. Excess liquid was absorbed with filter paper, and the grid was allowed to air dry. Grids were examined on a Zeiss EM10C transmission electron microscope (TEM) operating at an accelerating voltage of 100 kV.

2.3.4. Stressed tests

2.3.4.1. Centrifugal stress test. Metformin-loaded ghost RBCs and nanoerythrosomes were centrifuged at 1500, 3000, 4500, and 6000 rpm for 15 min at room temperature. The amount of leaked drug in the supernatant was determined with UV spectrophotometry.

2.3.4.2. Turbulence shock test. Metformin-loaded ghost RBCs and nanoerythrosomes were passed through subcutaneous gauge 23 syringes 5, 10, and 20 times and centrifuged at 3000 rpm for 10 min to determine the amount of leaked drug in the supernatant.

2.3.4.3. Osmotic shock test. 0.5 mL of nanoerythrosomes or ghost RBCs were incubated with 0.5 mL deionized water for 15 min at 4 °C. After that, samples were centrifuged at 3000 rpm for 10 min, and the amount of leaked drug in the supernatant was determined.

2.3.5. Long-term stability study

To investigate the stability of metformin-loaded nanoerythrosomes, for every concentration of loaded metformin and empty nanoerythrosomes, four factors including pH, conductivity, particle size (based on the number), and particle size (based on the volume) was obtained during 100 days, frequently. The samples were stored at 4 °C during the test. At the end of 100 days, the formulations were centrifuged at 3000 rpm for 10 min, and the amount of leaked drug was determined in the supernatant.

2.4. Drug content and loading parameters

Loading efficiency as the percentage of added drug loaded into nanoerythrosomes and loading capacity as the percentage of the weight of nanoerytheosomes that belongs to the drug were calculated from Equations (1) and (2).

Loading efficiency was measured through the indirect method by determining the amount of unloaded drug in the supernatant after the drug loading step. Loading capacity was measured after lyophilization of a known amount of nanoerythrosomes and weighing them.

$$Loading\ Efficiency = \frac{total\ amount\ of\ metformin - free\ metformin}{total\ amount\ of\ metformin} \times 100 \quad (1)$$

$$Loading\ Capacity = \frac{total\ amount\ of\ metformin - free\ metformin}{total\ weight\ of\ nanoerythrosome} \times 100 \quad (2)$$

2.5. Drug release and kinetic studies

We used the dialysis membrane method with a cut-off of 3.5 KDa to investigate drug release. 2 mL of metformin solution with 1 mg/mL concentration (as a control for evaluating probable effect of dialysis membrane on the release process) and the equivalent amount of metformin-loaded nanoerythrosomes was filled in a dialysis bag and floated in a PBS medium with pH = 7.4, T = 37 °C, and a stirring speed of 200 rpm. 3 mL of PBS medium was sampled at times of 0.5, 1, 2, 4, 6, 8, 10, 12, 24, and 30 h, and the released amounts of metformin were determined. After each sampling, an equal amount of PBS was replaced to maintain the sink condition.

For evaluating the kinetic of drug release, data attained from the release test was fitted to zero order, first order, Higuchi, Hixon-Crowell, and Korsmeyer-Peppas kinetic models. The accuracy and precision of the predicition of models were determined by sum of squared errors (SSE), the absolute percentage of error (E%), and the number of errors (NE%).

2.6. Metformin assay

UV/Vis spectrophotometry was used to determine the metformin amount. Based on the metformin UV absorbance spectrum, the λ_{max} was 233 nm. The method was validated by determining its linearity, precision based on interday and intraday variations, accuracy, and sensitivity. It is important that since the absorbance of the erythrocyte membrane had interferences with the λ_{max} of metformin (which is called the "matrix effect"), the same sample, without the drug, as a blank was used for every measurement (based on amounts and undergone processes) except we did not add metformin.

2.7. Statistical studies

Statistical repeated measure two-way analysis of variances (ANOVA) with Dunnet test as a post hoc for long-term stability, two-way ANOVA and Bonferroni post hoc for turbulence test, and for centrifugal stress test two-way ANOVA with Dunnet post hoc (GraphPad® Prism 9.2.0) were utilized to investigate the significance of observed data sets with p value < 0.05 as the significance level.

3. Results and discussion

It is shown that camouflaging nanoparticles with erythrocyte membranes would increase their brain concentration to 9–10 folds [46]. One study, showed that celecoxib-loaded nanoparticles entrapped in erythrocyte membrane had a better concentration in the brain than free drug or phospholipidic liposomes carrying celecoxib for the treatment of Alzheimer's disease [47]. Melnik et al. reported the exclusive effect of metformin on Wnt signaling in the glioma cell line. They showed that metformin inhibited Wnt pathway and caused lower expression of Sox4, which is responsible for a poor prognosis for the treatment of solid tumors [48]. Therefore, metformin can be promising for the treatment of glioma.

3.1. Nanoerythrosome preparation

To obtain ghost RBCs, a hypotonic treatment was used, a technique which is usually used for extracting RBCs' membranes [49]. Using hypotonic buffer and based on osmotic pressure, the contents of erythrocytes would be evacuated through its membrane pores. Repetition of this procedure during wash-outs would clear erythrocytes from their cytoplasm content and hemoglobin. This makes pale ghost RBCs which is observable in Fig. 3.

Ghost RBCs are ready for drug loading due to their open pores [50]. After incubation of drug solution and ghost RBCs, the addition of hypertonic buffer makes them plasmolysis, close their pores, and trap the drug inside them. The same method was used by Sun et al. which showed successful drug loading in RBCs [51]. Adding 1% of polysorbate 80 has been shown to absorb certain protein corona, which drives the nanoerythrosome toward LDL receptors of the BBB. This would help in brain targeting of nanoerythrosomes. Moreover, it was observed that polysorbate 80 modified the particle size distribution and particle size stability.

3.2. In-vitro characterizations

3.2.1. Particle size and particle size distribution

Based on measurements of DLS and PSA following particle sizes, as summarized in Tables 1 and 2, has been obtained. The important point is the difference in the measured size of each device. Since DLS measures the hydrodynamic diameter based on scattered light

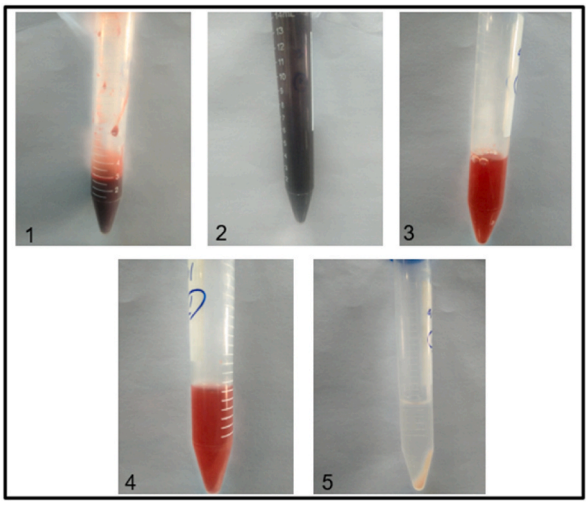

Fig. 3. The process of preparation of ghost RBCs.

Table 1
Results of DLS particle size measurement.

Representation of results	Drug loading	Mean D (nm)	D 10% (nm)	D 50% (nm)	D 90% (nm)	Z-average (nm)
Scattering light intensity	No	294.3 ± 46.6	117.1 ± 32.9	194.8 ± 55.4	737.8 ± 435.2	597.87 ± 300.84
Number		122.3 ± 38.4	104.5 ± 29.4	118.6 ± 36.2	145.7 ± 52.1	
Volume		136.2 ± 40.1	106.8 ± 31.2	127.1 ± 42.7	163.5 ± 61.7	
Scattering light intensity	Yes	137.4 ± 75.2	92.1 ± 33.8	127.9 ± 62.8	197.8 ± 141.6	307.00 ± 348.14
Number		97.1 ± 34.2	80.2 ± 25.0	93.5 ± 31.9	118.7 ± 46.3	
Volume		108.5 ± 43.0	84.0 ± 27.6	103.0 ± 38.4	140.3 ± 65.9	

Table 2
Results of PSA particle size measurement.

Representation of results	Drug loading	Median D (nm)	D 10% (μm)	D 90% (μm)	Mean D (μm)
Number	No	378 ± 270	309 ± 230	488 ± 298	391 ± 134
Volume		63.055 ± 548	14.869 ± 14.350	308.886 ± 425.024	49.791 ± 435
Number	Yes	664 ± 170	493 ± 364	1.007 ± 88	698 ± 149
Volume		24.252 ± 35.270	2.633 ± 3.287	41.680 ± 59.658	14.449 ± 43.955

during the time, and PSA works based on the amount and pattern of refracted light and measures laser diffraction equivalent diameter, a routine 20%–30% difference between their measurements is expected. Even though the difference between DLS and PSA particle size measurement for nanoerythrosomes is about 400%. This might be because of the biconcave shape of nanoerythrosomes, exactly like their ancestor erythrocytes. Since PSA measures the particle size only based on the cross-section of each particle, it sees them as larger particles. But DLS that analyzes the whole behavior can see its smaller overall size because of its concaveness on two sides. Interestingly, the SEM pictures of capecitabine-loaded nanoeryhtrosomes from the Nangare et al. study confirm our assumption [44]. Table 3 showed size distribution (span with PSA and PDI with DLS) of unloaded and loaded nanoerythrosomes.

3.2.2. Zeta potential

Based on the velocity and direction of nanoerythrosomes motion in electrophoresis, the zeta potential of unloaded- and loaded-nanoerythsosmes was −4.2 ± 2.0 mV and −4.2 ± 2.4 mV, respectively, which would be due the total loading of drug molecules inside erythrosomes. None of these have a significant difference with erythrocytes' zeta potential (−15 mV) which, to some extent, guarantees the free circulation of nanoerythrosomes in the blood without any interaction with other cells and biological components [52].

3.2.3. Shape and surface morphology

TEM results showed nano-size spherical nanoerythrosomes (Fig. 4). Although it seems that the spherical shape is interrupted by drug loading, this may be because of the interval time between nanoerythrosme preparation and taking the pictures. In the case of our hypothesis about the biconcave shape of nanoerythrosomes, even though we cannot count on the power of TEM for this conclusion, the contrast between borderlines and the middle of the nanoerythrosomes might be due to their RBC-like shape. Further studies, especially SEM imaging, are required to approve this assumption.

3.2.4. Stressed tests

Stressed tests are performed to give a view of the stability of the formulation during packaging, transportation, and administration. Moreover, these tests might investigate the effect of the bloodstream in its turbulences.

3.2.4.1. Centrifugal stress. The amount of leaked drug from both ghost RBCs and nanoerythrosomes in different centrifugal speeds is shown in Fig. 5. These amounts are negligible until 6000 rpm. Even at 6000 rpm, the leaked drug is less than 15% of the loaded drug. For nanoerythromes, the changes from 1500 to 6000 rpm did not significantly affect the amount of leaked drug. However, for ghost RBCs the amount of leaked drug at 6000 rpm was significantly higher than at 1500 rpm (p-value < 0.05).

Table 3
Indices of size distribution for nanoerythrosomes.

		Span	PDI
Unloaded nanoerythrosome	Scattering light intensity	3.289 ± 1.783	0.597 ± 0.215
	Number	0.330 ± 0.110	
	Volume	0.429 ± 0.152	
Loaded nanoerythrosomes	Scattering light intensity	0.654 ± 0.516	1.252 ± 1.468
	Number	0.382 ± 0.144	
	Volume	1.488 ± 0.270	

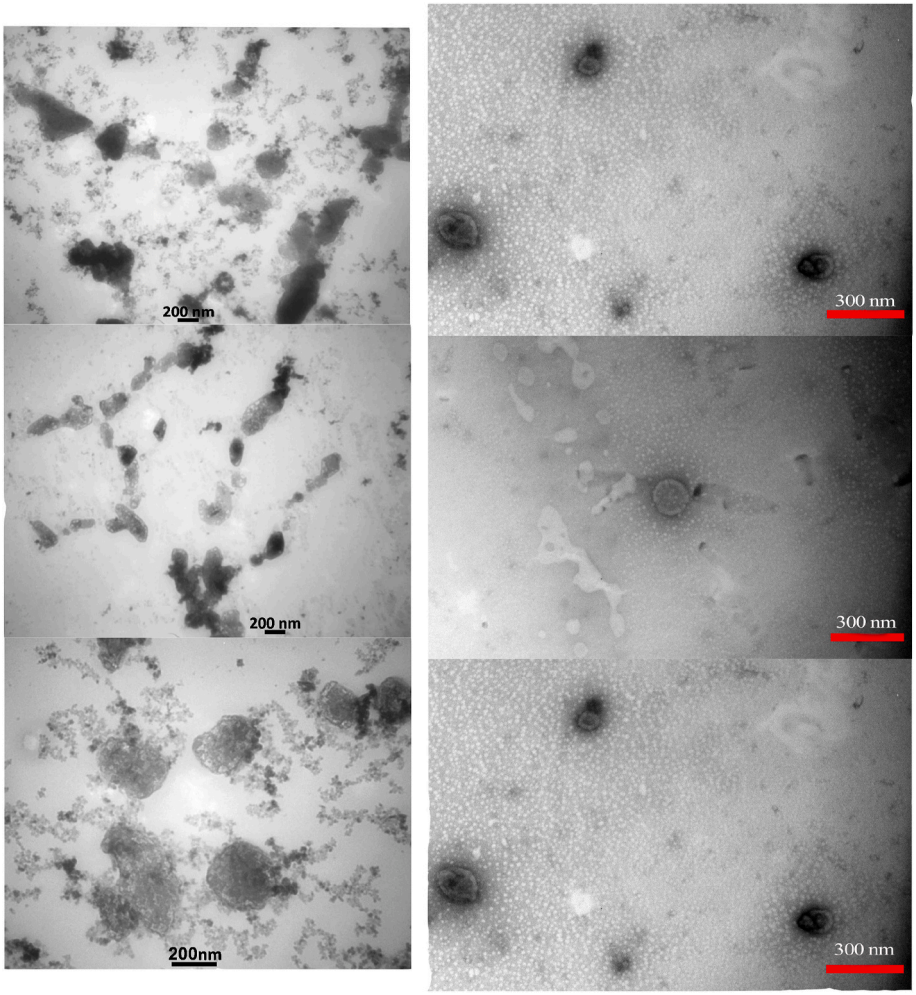

Fig. 4. TEM image of unloaded (right) and metformin-loaded (left) nanoerythrosomes.

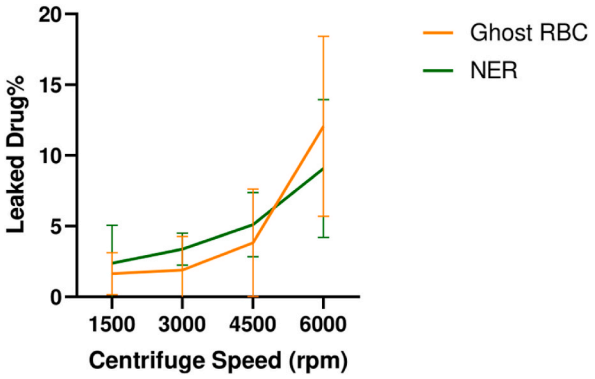

Fig. 5. The amount of leaked drug during centrifugal stress test.

3.2.4.2. Turbulence shock. This test resembles the flow of the ghost RBCs and nanoerythrosomes during administration through the syringe and its passages through vessels and capillaries. The test performed by using a syringe with smaller diameter than RBCs [53]. The amount of leaked drugs is shown in Fig. 6, which is not more than 10% of loaded drugs. No significant change was observed in any group (p-value > 0.05).

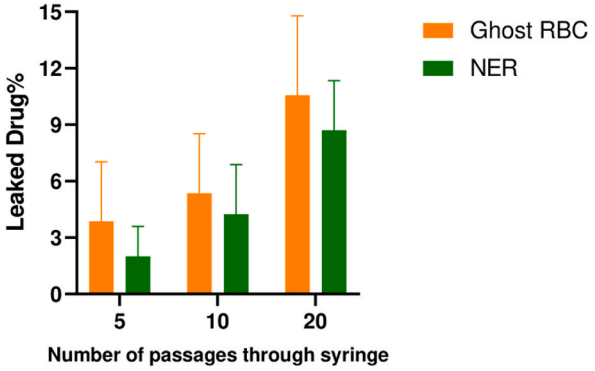

Fig. 6. The amount of leaked drug during turbulence shock test.

3.2.4.3. Osmotic shock. After 15 min of incubation of formulations with deionized water, the amount of leaked drug was 16.6% ± 22.54 and 13.63% ± 25.68 for nanoerythrosomes and ghost RBCs, respectively. Therefore, both nanoerythrosomes and ghost RBCs were almost resistant to osmotic shock.

3.2.5. Long-term stability

Based on Figs. 7–9, the variations of pH, conductivity, and particle size, based on the number and volume of the particles, have been investigated within 100 days. Similar to other studies, nanoerythrosomes are stable during the first-week pH-wise and size-wise. Regardless of the amount of metformin in nanoeryhtrosomes, their pH decreased, and conductivity increased with a similar slope. These alterations are due to the complex environment within nanoerythrosomes and remnants of cells which justify the traffic of different ions. However, there was no significant alteration in pH and conductivity after 100 days (except 1 mg/mL group). Particle sizes in both number and volume have increased during the first 20 days, because of the accumulation and agglomeration of nanoerythrosomes. After that, the reduction in particle size must be due to the destruction and degradation of nanoerythrosomes.

The amount of leaked drug from nanoerythrosomes after 100 days for 0.1 mg/mL, 1 mg/mL, and 10 mg/mL was 64.47% ± 41.86, 39.14% ± 41.88, and 9.91 ± 60.51, respectively (p-value < 0.05). This shows that nanoerythrosomes can maintain a reasonable amount of the loaded metformin inside their structure for a long time.

3.3. Drug content and loading parameters

Loading efficacy and loading capacity show the ability of the formulation to carry enough amounts of the drug. In Table 4 loading efficiency of nanoerythrosomes based on the concentration of metformin is summarized. By increasing the concentration of added metformin solution, loading efficiency decreases. It is because of the constant capability and space of nanoerythrosomes to load metformin. Nanoerythrosomes' loading capacity is calculated to be 1.66% which is the same as other studies worked with erythrosomes [54].

3.4. Drug release and kinetic modeling

As shown in Fig. 10, for free metformin, almost 95% of added drugs were released after 6 h. Metformin-loaded nanoerythrosomes have shown a well enough capability to conserve metformin inside their structure, and only 50% of the loaded drug has been released after 30 h. This shows that nanoerythrosome can preserve metformin until they reach the targeted site.

Based on the E% and AIC (the least error and AIC) [55] (Table 5), it can be concluded that Korsmeyer-Peppas is the best model that fits the pattern of metformin release from nanoerythrosomes, with the E% 0.076% and AIC -54.54. Based on the Korsmeyer-Peppas

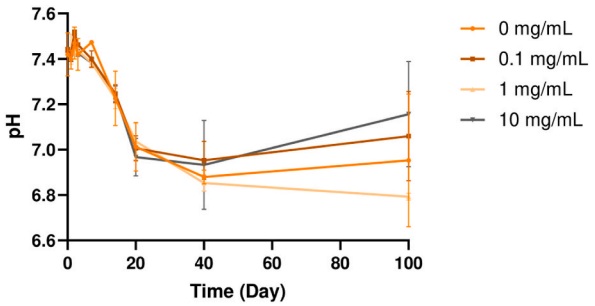

Fig. 7. Changes in pH of nanoerythrosomes during time.

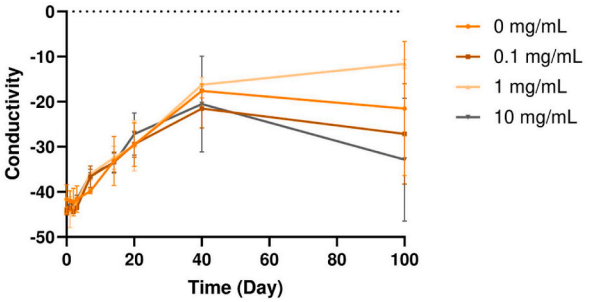

Fig. 8. Changes in conductivity of nanoerythrosomes during time.

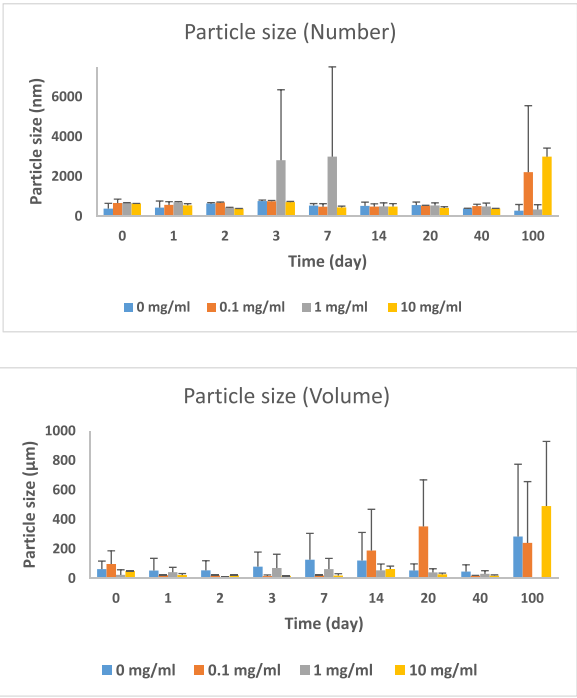

Fig. 9. Changes in particle size based on the number and volume of nanoerythrosomes during time.

Table 4
Loading efficiency of nanoerythrosomes in different concentrations of metformin.

Metformin concentration (μg/mL)	Loading efficiency %
100	72.60 ± 32.06
1000	27.17 ± 7.49
10,000	12.76 ± 1.22

formula ($F = K_{kp}t^n$) that F is the amount of released drug during time t, K_{kp} is a representative of the shape and structure of nanoparticles which is assumed to be 0.25 for spherical nanoparticles, and n is the release exponent. It is known that in the Korsmeyer-Peppas model for spherical particles, if n is less than 0.43, the dominant mechanism of release is diffusion [56]. This is compatible with our knowledge of nanoerythrosomes structure that consists of a cell membrane, and a drug would be entrapped inside it. The drug's release depends on its diffusion through this cell membrane.

3.5. Metformin assay

The linear regression (R^2) in the range of 1 μg/mL to 10 μg/mL was 0.99. The interday and intraday CV% and accuracy% are shown

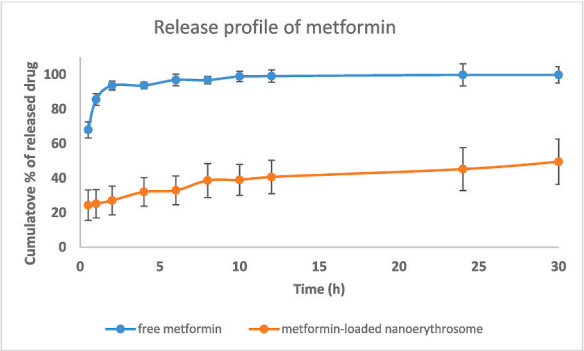

Fig. 10. The pattern of release for free metformin and metformin-loaded nanoerythrosome.

Table 5
Determinants of fitting of kinetic models to release data of metformin from nanoeythrosomes.

Model name	SSE	E%	AIC	NE%			
				5%	10%	12%	20%
Zero order	0.377	47.022	−5.775	0	0	0	0
First order	0.261	32.417	−9.417	0	10	10	20
Higuchi	0.101	19.807	−18.894	10	20	20	40
Hixon-Crowell	0.298	36.985	−8.102	0	0	0	10
Korsmeyer-Peppas	0.001	0.076	−54.540	70	100	100	100

to be less than 15% and in the range of 90%–110%, respectively. As indicators of sensitivity, the limit of detection (LOD) and the limit of quantification (LOQ) of our method has been calculated to be 1.06 μg/mL and 3.22 μg/mL, respectively.

4. Conclusion

Nanoerythrosomes are valuable carriers for metformin. Their ideal size, special shape, easy construction, suitable loading, biocompatibility, and capability to preserve the drug inside their structure are among the benefits of nanoerythrosomes. Moreover, since they should be made from the patient's blood, there would be no immunological or toxicological concern, which is a valuable step toward personalized medicine. Because of their enough loading space and large surface-to-volume ratio, they can deliver therapeutic doses of metformin to BBB, protect it from its metabolizing enzymes, and help it to cross the BBB to act there as an inhibitor of the Wnt signaling pathway to treat glioma. However, more studies including *in vivo* study to evaluate the ability of nanoerythrosome to pass the BBB, and an animal model of glioma to evaluate the efficacy of nanoerythrsome are needed. It is important to consider nanoerythrosomes flaws, too. Their low stability, special storage conditions, the impossibility of industrial manufacturing, weakness in loading of hydrophobic drugs, very low repeatability on construction and loading process, and their interference with analytical systems are among their problems that by solving them, we can achieve a powerful drug delivery system.

Author contribution statement

Seyed Mohammad Iman Moezzi: Performed the experiments; Wrote the paper.
Parisa Javadi: Analyzed and interpreted the data; Contributed reagents, materials, analysis tools or data.
Negin Mozafari, PhD: Analyzed and interpreted the data; Wrote the paper.
Hajar Ashrafi, PhD: Conceived and designed the experiments; Contributed reagents, materials, analysis tools or data; Wrote the paper.
Amir Azadi, ph.D.: Conceived and designed the experiments; Analyzed and interpreted the data; Contributed reagents, materials, analysis tools or data; Wrote the paper.

Data availability statement

Data will be made available on request.

Declaration of competing interest

The authors declare that they have no known competing financial interests or personal relationships that could have appeared to influence the work reported in this paper.

Acknowledgements

This article is the product of Pharm.D. dissertation of Seyed Mohammad Iman Moezzi, under supervision of Dr. Amir Azadi and Dr. Hajar Ashrafi. This study is performed under Grant number: 25812 afforded by Shiraz University of Medical Sciences and ethics certificate ID: IR.SUMS.REC.1401.253 followed by ARRIVE guidelines.

References

[1] R. Chen, M. Smith-Cohn, A.L. Cohen, H. Colman, Glioma subclassifications and their clinical significance, Neurotherapeutics 14 (2) (2017) 284–297.
[2] D.N. Louis, H. Ohgaki, O.D. Wiestler, W.K. Cavenee, P.C. Burger, A. Jouvet, B.W. Scheithauer, P. Kleihues, The 2007 WHO classification of tumours of the central nervous system, Acta Neuropathol. 114 (2) (2007) 97–109.
[3] L. Ding, Q. Wang, M. Shen, Y. Sun, X. Zhang, C. Huang, J. Chen, R. Li, Y. Duan, Thermoresponsive nanocomposite gel for local drug delivery to suppress the growth of glioma by inducing autophagy, Autophagy 13 (7) (2017 Jul 3) 1176–1190.
[4] Q.T. Ostrom, L. Bauchet, F.G. Davis, I. Deltour, J.L. Fisher, C.E. Langer, M. Pekmezci, J.A. Schwartzbaum, M.C. Turner, K.M. Walsh, M.R. Wrensch, The epidemiology of glioma in adults: a "state of the science" review, Neuro Oncol. 16 (7) (2014) 896–913.
[5] T.T. Lah, M. Novak, B. Breznik, Brain malignancies: glioblastoma and brain metastases, in: Seminars in Cancer Biology, Academic Press, 2020.
[6] X. Li, Y. Xiang, F. Li, C. Yin, B. Li, X. Ke, WNT/β-catenin signaling pathway regulating T cell-inflammation in the tumor microenvironment, Front. Immunol. 10 (2019) 2293.
[7] R. Nusse, H. Varmus, Three decades of Wnts: a personal perspective on how a scientific field developed, EMBO J. 31 (12) (2012) 2670–2684.
[8] M. McCord, Y.S. Mukouyama, M.R. Gilbert, S. Jackson, Targeting WNT signaling for multifaceted glioblastoma therapy, Front. Cell. Neurosci. 11 (2017) 318.
[9] T. Valenta, G. Hausmann, K. Basler, The many faces and functions of β-catenin, EMBO J. 31 (12) (2012) 2714–2736.
[10] R.K. Bikkavilli, S. Avasarala, M. Van Scoyk, J. Arcaroli, C. Brzezinski, W. Zhang, M.G. Edwards, M.K. Rathinam, T. Zhou, J. Tauler, S. Borowicz, Wnt7a is a novel inducer of β-catenin-independent tumor-suppressive cellular senescence in lung cancer, Oncogene 34 (42) (2015) 5317–5328.
[11] K.H. Kim, H.J. Seol, E.H. Kim, J. Rheey, H.J. Jin, Y. Lee, K.M. Joo, J. Lee, D.H. Nam, Wnt/β-catenin signaling is a key downstream mediator of MET signaling in glioblastoma stem cells, Neuro Oncol. 15 (2) (2013) 161–171.
[12] L.G. Morris, A.M. Kaufman, Y. Gong, D. Ramaswami, L.A. Walsh, Ş. Turcan, S. Eng, K. Kannan, Y. Zou, L. Peng, V.E. Banuchi, Recurrent somatic mutation of FAT1 in multiple human cancers leads to aberrant Wnt activation, Nat. Genet. 45 (3) (2013) 253–261.
[13] H. Zheng, H. Ying, R. Wiedemeyer, H. Yan, S.N. Quayle, E.V. Ivanova, J.H. Paik, H. Zhang, Y. Xiao, S.R. Perry, J. Hu, PLAGL2 regulates Wnt signaling to impede differentiation in neural stem cells and gliomas, Cancer Cell 17 (5) (2010) 497–509.
[14] T.I. Janjua, P. Rewatkar, A. Ahmed-Cox, I. Saeed, F.M. Mansfeld, R. Kulshreshtha, T. Kumeria, D.S. Ziegler, M. Kavallaris, R. Mazzieri, A. Popat, Frontiers in the treatment of glioblastoma: past, present and emerging, Adv. Drug Deliv. Rev. 171 (2021) 108–138.
[15] N. Auger, J. Thillet, K. Wanherdrick, A. Idbaih, M.E. Legrier, B. Dutrillaux, M. Sanson, M.F. Poupon, Genetic alterations associated with acquired temozolomide resistance in SNB-19, a human glioma cell line, Mol. Cancer Therapeut. 5 (9) (2006) 2182–2192.
[16] M. Latour, N.G. Her, S. Kesari, E. Nurmemmedov, WNT signaling as a therapeutic target for glioblastoma, Int. J. Mol. Sci. 22 (16) (2021) 8428.
[17] A.B. Fleming, W.M. Saltzman, Pharmacokinetics of the carmustine implant, Clin. Pharmacokinet. 41 (6) (2002) 403–419.
[18] J.C. Buckner, S.L. Pugh, E.G. Shaw, M.R. Gilbert, G. Barger, S. Coons, P. Ricci, D. Bullard, P.D. Brown, K. Stelzer, D. Brachman, Phase III study of radiation therapy (RT) with or without procarbazine, CCNU, and vincristine (PCV) in low-grade glioma: RTOG 9802 with Alliance, ECOG, and SWOG, Am. J. Clin. Oncol. (2014).
[19] M. Furuse, S. Kawabata, M. Wanibuchi, H. Shiba, K. Takeuchi, N. Kondo, H. Tanaka, Y. Sakurai, M. Suzuki, K. Ono, S.I. Miyatake, Boron neutron capture therapy and add-on bevacizumab in patients with recurrent malignant glioma, Jpn. J. Clin. Oncol. 52 (5) (2022 May) 433–440.
[20] N.A.O. Bush, S.M. Chang, M.S. Berger, Current and future strategies for treatment of glioma, Neurosurg. Rev. 40 (1) (2017) 1–14.
[21] J. Zhou, S. Massey, D. Story, L. Li, Metformin: an old drug with new applications, Int. J. Mol. Sci. 19 (10) (2018) 2863.
[22] D. Conza, P. Mirra, G. Calì, L. Insabato, F. Fiory, F. Beguinot, L. Ulianich, Metformin dysregulates the unfolded protein response and the WNT/β-Catenin pathway in endometrial cancer cells through an AMPK-independent mechanism, Cells 10 (5) (2021) 1067.
[23] H.T. Kwan, D.W. Chan, P.C. Cai, C.S. Mak, M.M. Yung, T.H. Leung, O.G. Wong, A.N. Cheung, H.Y. Ngan, AMPK activators suppress cervical cancer cell growth through inhibition of DVL3 mediated Wnt/β-catenin signaling activity, PLoS One 8 (1) (2013), e53597.
[24] G. Amable, E. Martínez-León, M.E. Picco, N. Di Siervi, C. Davio, E. Rozengurt, O. Rey, Metformin inhibits β-catenin phosphorylation on Ser-552 through an AMPK/PI3K/Akt pathway in colorectal cancer cells, Int. J. Biochem. Cell Biol. 112 (2019) 88–94.
[25] W. Yue, C.S. Yang, R.S. DiPaola, X.L. Tan, Repurposing of metformin and aspirin by targeting AMPK-mTOR and inflammation for pancreatic cancer prevention and treatment, Cancer Prev. Res. 7 (4) (2014) 388–397.
[26] C. Seliger, A.L. Meyer, K. Renner, V. Leidgens, S. Moeckel, B. Jachnik, K. Dettmer, U. Tischler, V. Gerthofer, L. Rauer, M. Uhl, Metformin inhibits proliferation and migration of glioblastoma cells independently of TGF-β2, Cell Cycle 15 (13) (2016) 1755–1766.
[27] M. Al Hassan, I. Fakhoury, Z. El Masri, N. Ghazale, R. Dennaoui, O. El Atat, A. Kanaan, M. El-Sibai, Metformin treatment inhibits motility and invasion of glioblastoma cancer cells, Anal. Cell Pathol. 2018 (2018).
[28] S. Valtorta, A.L. Dico, I. Raccagni, D. Gaglio, S. Belloli, L.S. Politi, C. Martelli, C. Diceglie, M. Bonanomi, G. Ercoli, V. Vaira, Metformin and temozolomide, a synergic option to overcome resistance in glioblastoma multiforme models, Oncotarget 8 (68) (2017), 113090.
[29] R.E. Kast, N. Skuli, G. Karpel-Massler, G. Frosina, T. Ryken, M.E. Halatsch, Blocking epithelial-to-mesenchymal transition in glioblastoma with a sextet of repurposed drugs: the EIS regimen, Oncotarget 8 (37) (2017), 60727.
[30] M.R. Welch, C. Grommes, Retrospective analysis of the effects of steroid therapy and antidiabetic medication on survival in diabetic glioblastoma patients, CNS Oncol. 2 (3) (2013) 237–246.
[31] C. Seliger, C. Luber, M. Gerken, J. Schaertl, M. Proescholdt, M.J. Riemenschneider, C.R. Meier, U. Bogdahn, M.F. Leitzmann, M. Klinkhammer-Schalke, P. Hau, Use of metformin and survival of patients with high-grade glioma, Int. J. Cancer 144 (2) (2019) 273–280.
[32] C. Seliger, E. Genbrugge, T. Gorlia, O. Chinot, R. Stupp, B. Nabors, M. Weller, P. Hau, Use of metformin and outcome of patients with newly diagnosed glioblastoma: pooled analysis, Int. J. Cancer 146 (3) (2020) 803–809.
[33] Y. Choi, M. Lee, Effects of enzyme inducers and inhibitors on the pharmacokinetics of metformin in rats: involvement of CYP2C11, 2D1 and 3A1/2 for the metabolism of metformin, Br. J. Pharmacol. 149 (4) (2006) 424–430.
[34] D.R. Harder, C. Zhang, D. Gebremedhin, Astrocytes function in matching blood flow to metabolic activity, Physiology 17 (1) (2002) 27–31.
[35] S. Miksys, Y. Rao, E.M. Sellers, M. Kwan, D. Mendis, R.F. Tyndale, Regional and cellular distribution of CYP2D subfamily members in rat brain, Xenobiotica 30 (6) (2000) 547–564.
[36] S. Javed, S. Alshehri, A. Shoaib, W. Ahsan, M.H. Sultan, S.S. Alqahtani, M. Kazi, F. Shakeel, Chronicles of nanoerythrosomes: an erythrocyte-based biomimetic smart drug delivery system as a therapeutic and diagnostic tool in cancer therapy, Pharmaceutics 13 (3) (2021 Mar 10) 368.
[37] K. Greish, Enhanced permeability and retention (EPR) effect for anticancer nanomedicine drug targeting, Cancer Nanotechnol. (2010) 25–37.
[38] R.H. Fang, A.V. Kroll, W. Gao, L. Zhang, Cell membrane coating nanotechnology, Adv. Mater. 30 (23) (2018), 1706759.
[39] J.S. Brenner, D.C. Pan, J.W. Myerson, O.A. Marcos-Contreras, C.H. Villa, P. Patel, H. Hekierski, S. Chatterjee, J.Q. Tao, H. Parhiz, K. Bhamidipati, Red blood cell-hitchhiking boosts delivery of nanocarriers to chosen organs by orders of magnitude, Nat. Commun. 9 (1) (2018) 1–14.
[40] J.S. Brenner, S. Mitragotri, V.R. Muzykantov, Red blood cell hitchhiking: a novel approach for vascular delivery of Nanocarriers, Annu. Rev. Biomed. Eng. 23 (2021) 225–248.

[41] E. Shtelman, A. Tomer, S. Kolusheva, R. Jelinek, Imaging membrane processes in erythrocyte ghosts by surface fusion of a chromatic polymer, Anal. Biochem. 348 (1) (2006) 151–153.
[42] F. Pierigè, S. Serafini, L. Rossi, M. Magnani, Cell-based drug delivery, Adv. Drug Deliv. Rev. 60 (2) (2008 Jan 14) 286–295.
[43] H. Yu, Z. Yang, F. Li, L. Xu, Y. Sun, Cell-mediated targeting drugs delivery systems, Drug Deliv. 27 (1) (2020 Jan 1) 1425–1437.
[44] S.A. Payghan, Nanoengineered erythrovesicles: camouflaged capecitabine as a biomimetic delivery platform, Asian J. Pharm. 11 (1) (2017).
[45] I. Samarzija, P. Sini, T. Schlange, G. MacDonald, N.E. Hynes, Wnt3a regulates proliferation and migration of HUVEC via canonical and non-canonical Wnt signaling pathways, Biochem. Biophys. Res. Commun. 386 (3) (2009) 449–454.
[46] Z. Chai, X. Hu, X. Wei, C. Zhan, L. Lu, K. Jiang, B. Su, H. Ruan, D. Ran, R.H. Fang, L. Zhang, A facile approach to functionalizing cell membrane-coated nanoparticles with neurotoxin-derived peptide for brain-targeted drug delivery, J. Contr. Release 264 (2017) 102–111.
[47] J.W. Guo, P.P. Guan, W.Y. Ding, S.L. Wang, X.S. Huang, Z.Y. Wang, P. Wang, Erythrocyte membrane-encapsulated celecoxib improves the cognitive decline of Alzheimer's disease by concurrently inducing neurogenesis and reducing apoptosis in APP/PS1 transgenic mice, Biomaterials 145 (2017) 106–127.
[48] S. Melnik, D. Dvornikov, K. Müller-Decker, S. Depner, P. Stannek, M. Meister, A. Warth, M. Thomas, T. Muley, A. Risch, C. Plass, Cancer cell specific inhibition of Wnt/β-catenin signaling by forced intracellular acidification, Cell Discov. 4 (1) (2018) 1–17.
[49] S. Melnik, D. Dvornikov, K. Müller-Decker, S. Depner, P. Stannek, M. Meister, A. Warth, M. Thomas, T. Muley, A. Risch, C. Plass, Red blood cell membrane camouflaged magnetic nanoclusters for imaging-guided photothermal therapy, Biomaterials 92 (2016) 13–24.
[50] L. Rao, B. Cai, L.L. Bu, Q.Q. Liao, S.S. Guo, X.Z. Zhao, W.F. Dong, W. Liu, Microfluidic electroporation-facilitated synthesis of erythrocyte membrane-coated magnetic nanoparticles for enhanced imaging-guided cancer therapy, ACS Nano 11 (4) (2017) 3496–3505.
[51] X. Sun, C. Wang, M. Gao, A. Hu, Z. Liu, Remotely controlled red blood cell carriers for cancer targeting and near-infrared light-triggered drug release in combined photothermal–chemotherapy, Adv. Funct. Mater. 25 (16) (2015) 2386–2394.
[52] F. Tokumasu, G.R. Ostera, C. Amaratunga, R.M. Fairhurst, Modifications in erythrocyte membrane zeta potential by Plasmodium falciparum infection, Exp. Parasitol. 131 (2) (2012) 245–251.
[53] D. Solanki, P. Sharma, M. Motiwale, L. Kushwah, RESEALLED erythrocytes: a BIOCARRIAR for drug delivery, World J. Pharm. Pharmaceut. Sci. 6 (4) (2017) 836–852.
[54] Y. Zhang, J. Zhang, W. Chen, P. Angsantikul, K.A. Spiekermann, R.H. Fang, W. Gao, L. Zhang, Erythrocyte membrane-coated nanogel for combinatorial antivirulence and responsive antimicrobial delivery against Staphylococcus aureus infection, J. Contr. Release 263 (2017) 185–191.
[55] N. Mozafari, A. Dehshahri, H. Ashrafi, S. Mohammadi-Samani, M.A. Shahbazi, R. Heidari, N. Azarpira, A. Azadi, Vesicles of yeast cell wall-sitagliptin to alleviate neuroinflammation in Alzheimer's disease, Nanomed.: NBM (NMR Biomed.) 44 (2022), 102575.
[56] P. Costa, J.M.S. Lobo, Modeling and comparison of dissolution profiles, Eur. J. Pharmaceut. Sci. 13 (2) (2001) 123–133.